LAWRENCE
LIVERMORE
NATIONAL
LABORATORY

LLNL-CONF-638803

Neural Interface for Deep Brain Stimulation

A. C. Tooker, T. E. Madsen, A. Crowell, K. G. Shah, S. H. Felix, H. S. Mayberg, S. S. Pannu, D. G. Rainnie, V. M. Tolosa

June 12, 2013

IEEE Neural Engineering
San Diego, CA, United States
November 5, 2013 through November 8, 2013

Disclaimer

Chronic, Multi-Contact, Neural Interface for Deep Brain Stimulation

Angela Tooker, Teresa E. Madsen, Andrea Crowell, Kedar G. Shah, Sarah Felix, Helen S. Mayberg, Satinderpall Pannu, Donald G. Rainnie, Vanessa Tolosa

***Abstract*— Recent clinical studies show deep brain stimulation (DBS) as a promising therapy for the chronic treatment of major depression. Although an increasing number of studies have shown the clinical benefits of DBS in patients with major depressive disorder, little is known about the underlying mechanisms by which the treatment works. The neural interface described here consists of two multi-contact, polymer-based, microelectrode arrays that were specially-designed and fabricated. The first is for stimulation of the medial prefrontal cortex (mPFC) and the second is for recording local field potentials (LFPs) and event related potentials (ERPs) in the basolateral amygdala (BLA). Unlike conventional metal wire stimulating arrays, this stimulating array offers 144 spatial configurations, both monopolar and bipolar. We present here preliminary results involving stimulation of various contact points spanning the mPFC, with simultaneous recording from multiple contacts across the temporal lobe.**

I. Introduction

Deep brain stimulation (DBS) as a therapeutic option has been FDA-approved for the treatment of essential tremor, and Parkinson's disease. With promising clinical trials for diseases such as obsessive-compulsive disorder, Alzheimer's, dystonia, and epilepsy, the patient population treated with DBS is expected to grow [1-3]. Major depressive disorder has also emerged as another neuropsychiatric disorder to benefit from DBS [4-5]. Despite the clinical successes, however, the biological mechanisms of DBS are still unknown. As the mechanisms are likely specific to both the disease and the stimulation parameters/location, investigating the mechanisms of DBS treatment for different disorders will likely require a flexible platform with a variety of different sensing/stimulating modalities.

Investigations into the neurobiology and brain circuitry underlying the mechanisms of DBS treatment for depression have been limited, partly by the neuro-technologies available. Standard metal wire stimulating electrodes only allow a single stimulation site per animal, with no control over position or current spread after implantation. A commitment to either monopolar or bipolar stimulation is made even earlier, as they require different electrode structures (a ground wire wrapped around a skull screw, as opposed to a bipolar concentric stimulating electrode). Therefore, only one configuration per animal is possible, and all comparisons of different conditions must be made between animals introducing high variability. The development of neuro-technologies with larger numbers of electrodes, capable of a wide range of stimulus parameters, will further contribute towards an understanding of the mechanisms underlying DBS and may result in more effective stimulation.

Micro-fabricated, multi-contact, polymer-based electrode arrays are well-suited to overcome these challenges [6-10]. These arrays can be fabricated with large numbers of variously-sized electrodes, suitable for recording or stimulating at very specific locations in the brain. They can be easily interfaced with commercially-available stimulating and recording equipment. Further, a single microelectrode array can be used with a wide variety of stimulus options, both bipolar and monopolar.

Multiple studies have now demonstrated the effectiveness of stimulation of subcallosal cingulate region, specifically adjacent to the Brodmann area (BA) 25, for treatment of depression. In the rat, the ventromedial prefrontal cortex (vmPFC) has been suggested to be homologous to the human BA 25, and stimulation of the vmPFC has been tested in rat models of depression [11]. However, the rat vmPFC can be further divided into the infralimbic and prelimbic cortex, each of which has distinct patterns of anatomic connectivity, including different projections to the amygdala [12]. They also have dissociable, sometimes opposing, effects on fear conditioning [13] and on response to the forced swim test, an animal model of depression [14]. Independent stimulation of these areas, while recording the electrophysiological response from an anatomical target involved in emotion regulation and expression, together with simultaneous behavioral observation provides a powerful way to further investigate the therapeutic mechanism of DBS.

We present here results from an investigation of electrical stimulation and electrophysiological recording in a freely moving rat using a microfabricated polymer-based neural interface. The neural interface is customized to stimulate across 12 different contacts within the mPFC and simultaneously record LFPs and single units (spikes) across the temporal lobe. Preliminary analysis show marked differences in response across the temporal lobe depending on stimulation contacts and other factors, providing support

*Research supported by Lawrence Livermore National Laboratory.

A. Tooker is with Lawrence Livermore National Laboratory, Livermore, CA 94550 USA (phone: 925-422-2326; e-mail: tooker1@llnl.gov).

K. Shah, S. Felix, S. Pannu, and V. Tolosa are with Lawrence Livermore National Laboratory, Livermore, CA 94550 USA (e-mail: shah22@llnl.gov, felix5@llnl.gov, pannu1@llnl.gov, tolosa1@llnl.gov).

T.E. Madsen, A. Crowell, and D.G. Rainnie are with Emory University School of Medicine, Atlanta, GA (email: tmadsen@emory.edu, andrea.crowell@emory.edu, drainni@emory.edu)

H.S. Mayberg is with Department of Psychiatry, Emory University, Atlanta, GA (email: hmayber@emory.edu)

for the benefits of a multi-contact microelectrode neural interface.

II. Design and Fabrication

The neural interface is specially-designed for use in rats. It is however, scalable for use in a wide variety animals, including humans. It consists of two separate electrode arrays: one optimized for stimulating and the other optimized for recording.

A. Stimulating Electrode Array Design

This first electrode array is designed for electrical stimulation of the medial prefrontal cortex (mPFC). The two main design considerations for this array were 1) large electrical contacts (0.06 mm^2) and 2) an implantable length of at least 6 mm. The array has 12 stimulating electrodes, each 150 µm by 400 µm (Figure 1). The electrodes are arranged in two rows, with a center-to-center spacing of 600 µm within each row and a center-to-center spacing of 200 µm between rows. There are also four small electrodes at the tip of this array, designed for future use as electrochemical sensors [6].

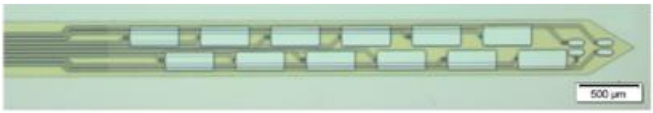

Figure 1. Image of the stimulating electrode array. The twelve stimulating electrodes are each 150 µm by 400 µm. The four small electrodes at the right of the probe are designed for future use as electrochemical sensors.

B. Recording Electrode Array Design

The second electrode array is designed for recording local field potentials (LFPs) and event related potentials (ERPs) in the basolateral amygdala (BLA). The primary design considerations for this array were: 1) an implantable length of at least 10 mm, 2) multi-shank, and 3) an extra-large reference electrode (> 0.3 mm^2). The array has 4 individual shanks, each with 4 recording electrodes (Figure 2). The electrodes are 50 µm in diameter with a center-to-center spacing of 800 µm. The shank width is 218 µm and the separation between the shanks is 582 µm. The implantable region for this device is 11 mm. There is a reference electrode (150 µm by 2000 µm) on one of shanks.

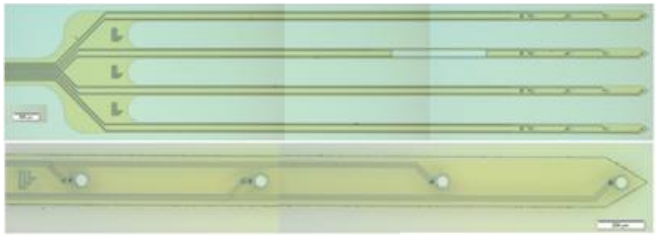

Figure 2. Images of the recording electrode arrays. The top image shows four individual shanks. The second shank from the top has the extra-large recording electrode. The bottom image shows an enlargement of one of the shanks. Each shank has four electrodes, 50 µm in diameter.

C. Electrode Array Fabrication

Both the stimulating and recording arrays undergo the same fabrication process. These are polyimide-based arrays utilizing three layers of trace metal (gold) and a separate electrode metal layer (iridium). A cross-section of the final device is shown in Figure 3, the full fabrication process is described elsewhere [7].

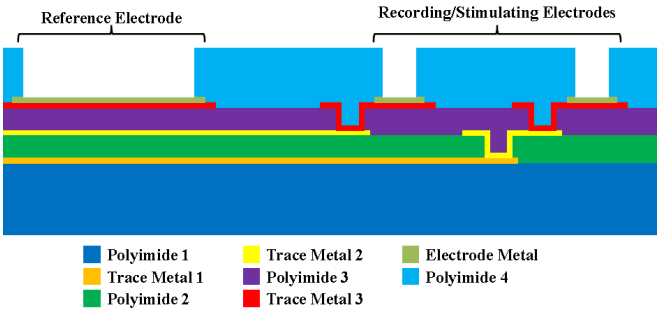

Figure 3. Schematic of the final electrode array cross-section. Both the stimulating and recording arrays utilize the same fabrication process (although the stimulating array does not have a reference electrode).

Upon completion of the device fabrication, electrical connectors, ground wires, and insertion stiffeners are attached (Figure 4). Standard Omnetics connectors (Omnetics Connector Co., Minneapolis, MN) are attached to the polyimide electrode array. A ground wire is also attached directly to the polyimide array. The Omnetics connector and ground wire allow these devices to interface directly with a wide variety of commercially-available stimulation and recording equipment. As these polyimide arrays tend to buckle upon insertion into neural tissue, custom-designed insertion stiffeners were utilized [15]. The silicon insertion stiffeners are specially-designed to mate with either the stimulating or recording array. At one end of the insertion stiffener there is a large tab, which allows for easy handling without contacting the attached array. The stiffeners are fabricated using standard silicon processing techniques. The array and stiffener can be easily aligned to within 10 µm using a flip-chip bonder.

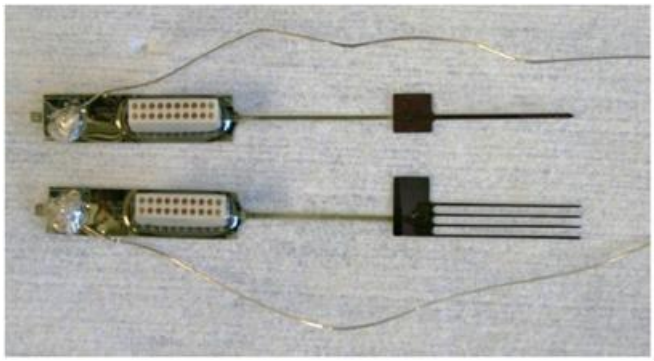

Figure 4. Images of electrode arrays with Omnetics connectors, ground wires, and insertion stiffeners attached. The top device is the stimulating electrode array and the bottom device is the recording array.

III. Results

A. In Vitro *Electrical Characterization*

The iridium electrodes were activated using biphasic potential pulsing in phosphate-buffered saline to form an activated iridium-oxide film (AIROF). All electrodes were characterized to determine the charge-storage-capacity (CSC) and impedance. Cyclic voltammetry and electrochemical impedance measurements were made with a Princeton Applied Research (PAR) potentiostat using vendor-supplied software. The average CSC for the 12 stimulating contacts is

20.17 ± 0.2 mC/cm^2, with an average impedance of 1.9 ± 0.1 kΩ at f = 1 kHz. For the 16 recording contacts, the average impedance is 6.3 ± 0.1 kΩ at f = 1 kHz.

B. In Vivo *Neural Stimulation and Recording*

An adult Harlan Sprague-Dawley rat weighing approximately 400g was chronically implanted with both a stimulating and a recording electrode. The stimulating electrode was implanted in the right mPFC (AP: +2.7, ML: -1.12, DV: -5.91, 6° lateral approach angle), with the intention of covering the infralimbic and prelimbic portions. The four-shank recording electrode was implanted in the ipsilateral basolateral amygdala (AP: -3.0, ML: -3.59, DV: -9.83, 6° medial approach angle). Craniotomies were sealed with KwikSil (World Precision Instruments, Sarasota, FL) and probes were fixed in position with dental acrylic and superglue. The flexible polyimide cable was then coated in KwikSil to help avoid kinking during final positioning and fixation of the Omnetics connector in the acrylic headcap.

After one week of surgical recovery, acute stimulation with simultaneous recording was performed in the awake, freely-moving rat, typically over a period of 75-150 minutes per day.

In contrast to commercially available stimulating electrodes, the multi-contact electrode arrays presented here offer 144 possible spatial configurations (12 monopolar + 12x11 bipolar pairs, including reversed polarities), allowing within-subject comparisons. All of this flexibility, of course, runs the risk of seriously overcomplicating the experimental design. Thus, as an initial exploratory pilot experiment, we chose to stimulate mostly adjacent pairs of electrodes across the full extent of the array. We expected to find differential responses to stimulation in the Prelimbic Cortex (PrL) and Infralimbic Cortex (IL), which have distinct patterns of reciprocal connectivity with different parts of the amygdala. Figure 5 shows the event related potentials (ERPs) recorded in the BLA in response to 2 Hz, 0.45 mA stimulation pulses on 14 bipolar electrode configurations, in random order. Using the color-coded topography at right, we can see that the ERP waveforms tend to cluster by anatomical position of the active stimulation site. Specifically, the yellow/green range of stimulation sites is notable for its strong negative component of the ERP around 50-80 ms, especially at the dorsal recording contact (AD15), and the blue/black range shows a strong positive component around 100-160 ms, especially on the more ventral recording contact (AD16). The red/gray range has relatively small ERPs, blending into noise, which likely reflects that those contacts were situated in the dorsal mPFC region Cg1, which is less intimately interconnected with the amygdala.

The two recording contacts selected for analysis here, because of their large ERPs with representatively distinct patterns, are both located on a single shaft, separated by 1.6 mm. The ERPs measured across the entire 2.4 mm by 2.4 mm distribution of recording sites are noticeably different, suggesting that they are indeed spread across various nuclei of the amygdala and surrounding temporal cortices. Inferences may be drawn especially from the latency at which ERP deflections are first observed, as it has been shown in cats that antidromic activation of BLA projections to mPFC fire with shorter latency (8-23 ms) than orthodromic activation of BLA neurons by projections from mPFC (35-40 ms) [16]. Those values are similar to the two earliest peaks in AD15 (Figure 5), albeit slightly slower owing to the larger brains.

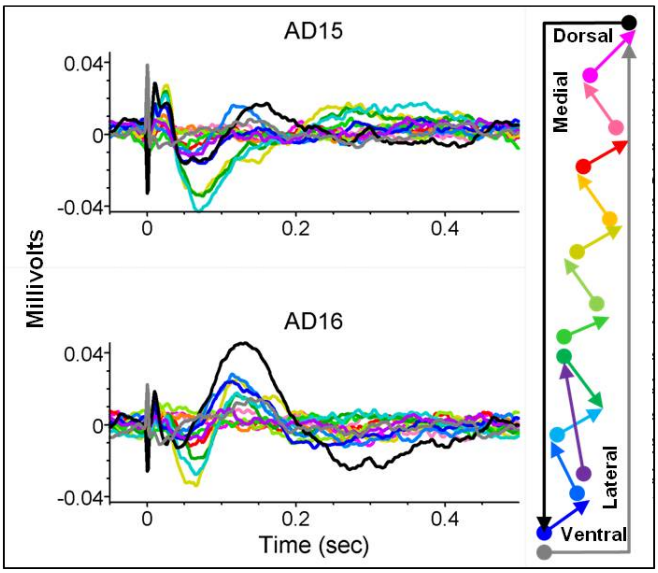

Figure 5. Event Related Potentials on the stimulating electrode arrays. LFPs recorded from two selected contacts on the amygdala array, triggered by each mPFC stimulation artifact (at time 0), and averaged across 3 minutes of 2 Hz, 0.45 mA stimulation in 14 different bipolar configurations. The schematic at right gives an approximate color-code for the spatial arrangement of the stimulated pairs, wherein the arrowhead indicates the active (-) contact, while the circle indicates the ground (+) contact.

Following that survey of mostly adjacent contact pairs, it was noticed that one of the largest and earliest responses came from stimulation of the most distal pair of electrodes. Furthermore, the polarity was critical, as stimulation with the most ventral contact as the active (-) electrode and the most dorsal contact as the ground (+) electrode produced the largest positive component of the ERP (black), while the reverse polarity stimulation of the same pair had a minimal ERP (gray), despite an equally large, mirror image stimulation artifact. Thus, the next experiment was to keep either the ventral active (-) contact or the dorsal ground (+) contact constant, while varying the other in random order. Thus, the spatial configurations of interest were narrowed down to two, on which we explored higher frequencies of stimulation, to gain a better understanding of the mechanisms at play in a clinical DBS application.

Figure 6 represents a preliminary experiment in which the frequency was increased from 2 Hz to 4, 8, and finally 20 Hz. Other experiments have since progressed all the way to the clinically applicable 130 Hz, and reversed the progression of frequencies back down to 2 Hz. Notice how 2 Hz stimulation initiates a damped oscillation around 5-8 Hz, which is the same range as BLA projection neuron's resonant frequencies. In fact, it seems that specific recording sites across the array have distinct frequencies at which they prefer to respond, reflected in the ERP

waveforms. Overall, there is a tendency for the ERPs to entrain easily to stimulation at or below the resonant frequency, but get disrupted, such that there is almost no significant ERP, when stimulated above the recording site's preferred frequency. Albeit preliminary, this finding could hint at a possible therapeutic mechanism for DBS. We and others have demonstrated the central role of low frequency (2-4 Hz) oscillations in fear learning and expression [17-18]. If this can be generalized to other forms of negative affect, it seems plausible that high frequency DBS may disrupt the limbic network's ability to organize at such low frequencies.

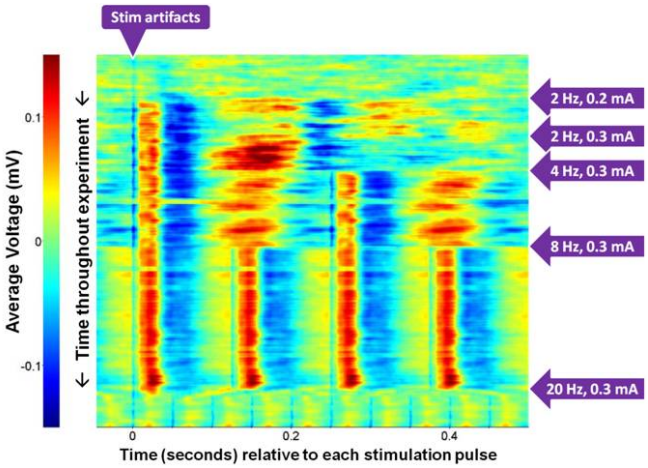

Figure 6. ERPs over time, with increasing stimulation frequency. Stimulation artifact triggered average of a single LFP (AD15), with the recorded voltage, now reflected by color, as a slower (experimental) timescale is added to the Y axis. Each row reflects the ERP calculated over a sliding window of a few minutes. The relative times of experimental manipulations to the stimulation current and frequency can be seen at the right.

IV. Conclusion

We present here the results from the initial studies using this multi-contact, microelectrode, neural interface. The preliminary results show that there is a marked difference in response across the temporal lobe depending upon the stimulation parameters, especially the spatial configuration of electrodes and the stimulation frequency.

This current neural interface is a chronic implant, capable of electrical stimulation and recording in a freely moving animal for at least 7 weeks. Future versions will incorporate targeted drug delivery and electrochemical sensing on a single, integrated neural interface.

Acknowledgment

This work has been funded by Lawrence Livermore National Laboratory. This work performed under the auspices of the U.S. Department of Energy by Lawrence Livermore National Laboratory under Contract DE-AC52-07NA27344. LLNL-CONF-638803

References

[1] B. Greenberg, D. Malone, G. Friehs, A. Rezai, C. Kubu, P. Malloy, S. Salloway, M. Okun, W. Goodman, and S. Rasmussen, "Three-year outcomes in deep brain stimulation for highly resistance obsessive-compulsive disorder," *Neuropsychopharm.*, vo. 31, pp. 2384-2393, 2006.

[2] A.W. Laxton, D.F. Tang-Wai, M.P. McAndrews, D. Zumsteg, R. Wennberg, R. Keren, J. Wherrett, G. Naglie, C. Hamani, G.S. Smith, and A.M. Lozano, "A phase I trial of deep brain stimulation of memory circuits in Alzheimer's disease," *Annals Neurology*, vol. 68, no. 4, pp. 521-534, 2010.

[3] T. Loddenkemper, A. Pan, N. Silvia, K. Baker, A. Rezai, S. Dudley, E. Montgomery, and H. Luders, "Deep brain stimulation in epilepsy," *J. Clin. Neurophys.*, vol. 18, no. 6, pp. 514-532, 2001.

[4] H. Mayberg, A. Lozano, V. Voon, H. McNeely, D. Seminowicz, C. Hamani, and J. Schwalb, "Deep brain stimulation for treatment-resistance depression," *Neuron*, vol. 45, no. 5, pp. 651-660, 2005.

[5] R. Anderson, M. Frye, O. Abulseoud, K. Lee, J. McGillivray, M. Berk, and S. Tye, "Deep brain stimulation for treatment-resistant depression: Efficacy, safety, and mechanisms of action," *Neurosci. Biobehavioral Rev.*, vol. 36, no. 8, pp. 1920-1933, 2012.

[6] A. Tooker, T.E. Madsen, A. Yorita, A. Crowell, K.G. Shah, S. Felix, H.S. Mayberg, S. Pannu, D.G. Rainnie, and V. Tolosa, "Microfabricated Polymer-Based Neural Interface for Electrical Stimulation/Recording, Drug Delivery, and Chemical Sensing – Development," in *Proc. 35th IEEE Eng. Med. Biol. Soc. Ann. Int. Conf. 2013*, to be published.

[7] A. Tooker, V. Tolosa, K.G. Shah, H. Sheth, S. Felix, T. Delima, and S. Pannu, "Optimization of Multi-Layer Metal Neural Probe Design," in *Proc. 34th IEEE Eng. Med. Biol. Soc. Ann. Int. Conf. 2012*, California, USA, August 2012.

[8] B. Rubehn, C. Bosman, R. Oostenveld, P. Fries, and T. Stieglitz, "A MEMS-based flexible multi-channel ECoG-electrode array," *J. Neural Eng.*, vol. 6, no. 3, June 2009.

[9] A. Mercanzini, K. Cheung, D. Buhl, M. Boers, A. Maillard, P. Colin, J.-C. Bensadoun, A. Bertsch, and P. Renaud, "Demonstration of cortical recording using novel flexible polymer neural probes," *Sens. Actuators A*, vol. 143, pp. 90-96, 2008.

[10] J. Seymour, N. Langhals, D. Anderson, and D. Kipke, "Novel multi-side, microelectrode arrays for implantable neural applications," *Biomed. Microdevices*, vol. 13, pp. 441-451, February 2011.

[11] C. Hamani, M. Diwan, C.E. Macedo, M.L. Brandao, J. Shumake, F. Gonzalez-Lima, R. Raymond, A.M. Lozano, P.J. Fletcher, and J.N. Nobrega, "Antidepressant-like effects of medial prefrontal cortex deep brain stimulation in rats," *Biol. Psych.*, vol. 67, no. 2, pp. 117-124, 2010.

[12] R. Vertes, "Differential projections of the infralimbic and prelimbic cortex in the rat," *Synapse,* vol. 51, pp. 32-58, 2004.

[13] D. Sierra-Mercado, N. Pailla-Coreano, G.J. Quirk, "Dissociable roles of prelimbic and infralimbic cortices, ventral hippocampus, and basolateral amygdala in the expression and extinction of conditioned fear," *Neuropsychopharm,* vol. 36, pp. 529-538, 2011.

[14] C. Hamani, M. Diwan, S. Isabella, A.M. Lozano, J.N. Nobrega, "Effects of different stimulation parameters on the antidepressant-like response of medial prefrontal cortex deep brain stimulation in rats," *J. Psychiatr. Res.*, vol. 44, pp. 683-687, 2010.

[15] S. Felix, K.G. Shah, D. George, V. Tolosa, A. Tooker, H. Sheth, T. Delima, and S. Pannu, "Removable Silicon Insertion Stiffeners for Neural Probes using Polyethylene Glycol as a Biodissolvable Adhesive," in *Proc. 34th IEEE Eng. Med. Biol. Soc. Ann. Int. Conf. 2012*, California, USA, August 2012.

[16] E. Likhtik, J.G. Pelletier, R. Paz, and D. Pare, "Prefrontal Control of the Amygdala," *J. Neurosci.*, vol. 25, no. 32, pp. 7429-7437, August 2005.

[17] S.J. Ryan, D.E. Ehrlich, A.M Jasnow, S. Daftary, T.E. Madsen, and D.G. Rainnie, "Spike-Timing Precision and Neuronal Synchrony Are Enhanced by an Interaction between Synaptic Inhibition and Membrane Oscillations in the Amygdala," *PLos One*, vol. 7, no. 4, April 2012.

[18] H.-C. Pape and D. Pare, "Plastic Synaptic Networks of the Amygdala for the Acquisition, Expression, and Extinction of Conditioned Fear," *Physiol. Rev.*, vol. 90, pp. 419-463, 2010.